ISSN: 2350-0328

International Journal of Advanced Research in Science, Engineering and Technology

Vol. 6, Issue 8 , August 2019

Methods of Improving the Accuracy of Electromagnetic Flowmeters with Low Frequency Pulsed Power of the Inductor

Yusupbekov Nodirbek Rustambekovich, Jumaev OdilAbdujalilovich, NormurodovJahongirNormurodogli

Professor, Electronics and Automation Faculty, Tashkent State Technology University, Tashkent, Uzbekistan
Associate Professor, Automation Faculty, NavoiState Mining Institute, Navoi, Uzbekistan
Assistant Professor, Automation Faculty, NavoiState Mining Institute, Navoi, Uzbekistan

ABSTRACT: The article discusses methods to improve the accuracy of the measuring channels and the electromagnetic flowmeter as a whole. Analyzed are the spectral densities of the resulting thermal noise of the converter with the representation of the curves of the moduli of the frequency characteristic of the conversion path for noise at various integration times that determine the frequency domain, the noise in which passes with the greatest weight to the output of the conversion path. The most significant factors limiting the accuracy of the flowmeter set with a low level of the output signal of the conversion circuit, the causes of intrinsic noise in the conversion path, and their elimination methods are analyzed. Algorithms are proposed for calculating the noise components of the input amplifier for the optimal choice of the method and parameters of analog-to-digital conversion and the type of input operational amplifier that allow resolving the contradiction between accuracy and power consumption of the inductor.

KEY WORDS: Flowmeter, flow control, analog-to-digital converter dynamic range, spectral density, reliability, measurement accuracy, converter, inductor power, noise, magnetic induction.

I.INTRODUCTION

Existing flowmeters are very diverse both in the design of the primary transducers and in the measuring circuits used. Electromagnetic flowmeters are widely used to measure and control liquids, which are caused by a number of advantages of such flowmeters: There are no moving parts in the design of electromagnetic sensors. The sensor does not contain parts that create resistance to flow. They are chemically resistant to almost any kind of liquid and are independent of the readings on viscosity, pressure, temperature, density or conductivity.

Especially with the development of microprocessor tools and their implementation in information-measuring systems, as well as the use of programmable process control and measurement digital processing with pulsed low-frequency inductor power in electromagnetic flowmeters, the metrological characteristics of electromagnetic flowmeters dramatically increase.

II. SIGNIFICANCE OF THE SYSTEM

The task of improving the accuracy of an electromagnetic flowmeter is achieved by the fact that in this flowmeter the power is supplied by bipolar pulses with a pause frequency of 5 Hz. Powering the sensor with a bipolar flow, ceteris paribus, gives the sensitivity doubled. Moreover, when using pulsed power, it becomes possible to significantly simplify both the electromagnetic sensor and the measuring circuit.

III. LITERATURE SURVEY

However, reducing the energy consumption of the flowmeter by reducing the power supply to the inductor leads to a decrease in the primary transducers of the output emf, since the output emf of the primary transducer directly changes the magnetic field induction. In this connection, the task of developing electronic converters for electromagnetic flowmeter (CEM) operating at very low levels of input signals becomes urgent, which, accordingly, requires an analysis of the specific features of such converters and an assessment of the factors limiting their accuracy.

ISSN: 2350-0328
International Journal of Advanced Research in Science, Engineering and Technology
Vol. 6, Issue 8 , August 2019

Choosing an integrating ADC method with an integration time in conversion schemes that are multiple to the interference period, one can almost completely eliminate the influence of the periodic interference of the induced supply circuit [3].

IV. METHODOLOGY

Thus, one of the most significant factors limiting the accuracy of the flowmeter set at a low output level of the conversion circuit is the influence of the intrinsic noise of the primary converter pertaining to thermal noise and is caused by the difference in PC as a signal source equivalent to internal resistance R3 (resistance of fluid mass between electrodes). This noise occurs in any circuit having an equivalent active resistance, and its value depends only on the resistance value and does not depend on the physical nature of the noise source [4]. The spectral density of thermal noise does not depend on frequency. The noise of the operational amplifier is characterized by the noise voltages and currents brought to the input, having a spectral power density of $s_U(\omega)$ and $s_I(\omega)$, respectively. The total power spectral density of the equivalent total voltage noise, reduced to the CEM input, will be [5]:

$$s(\omega) = s_U(\omega) + s_I(\omega){R_a}^2 + 4kTR_э$$

where k is the Boltzmann constant; T is the absolute temperature; ω is the angular frequency.

In this ratio, the first two members of the right-hand side are the noise of the CEM input amplifier, the third is the noise of the PC.

By the form of the dependence of the spectral density on the frequency, the PC noise is white noise, the noise of the input amplifier has two components — white noise and flicker noise, while the dependence of both S_U and S_I on the frequency ω is

$$S_U = S_{U^0}\left(1 + \frac{\omega_0}{\omega}\right);$$

$$S_I = S_{I^0}\left(1 + \frac{\omega_0}{\omega}\right),$$

where S_{U^0}, S_{I^0} characterize the amount of white noise; ω_0 is the frequency, below which flicker noise prevails [5].

The frequency ω_0 for current noise is usually higher than for voltage noise. Passing through the CEM conversion scheme, the noise spectrum will change in accordance with the frequency response of the conversion scheme, which is determined by the conversion method and the timing diagram parameters.

In fig. 1a, a time diagram of one period of current in the inductor is shown with bipolar pulsed power normally used at present. The output voltage PC contains a component of the useful signal, proportional to the magnetic induction, and negatively, the current supply of the inductor, and the component of the transformer interference, proportional to the derivative of the current inductor. In fig. 1 moment t_1-corresponds to the inclusion of the inductor current of positive polarity; t_2-the beginning of the measurement interval signal PC positive polarity; t_3 - the end of the measurement interval of the signal PC of positive polarity and the beginning of the trailing edge of the pulse; t_4-turn on the inductor current of negative polarity; t_5 is the beginning of the measurement interval of the PP signal of negative polarity; t_6 is the end of the measurement interval of the signal PC of negative polarity and the beginning of the trailing edge of the pulse.s

ISSN: 2350-0328
International Journal of Advanced Research in Science, Engineering and Technology
Vol. 6, Issue 8 , August 2019

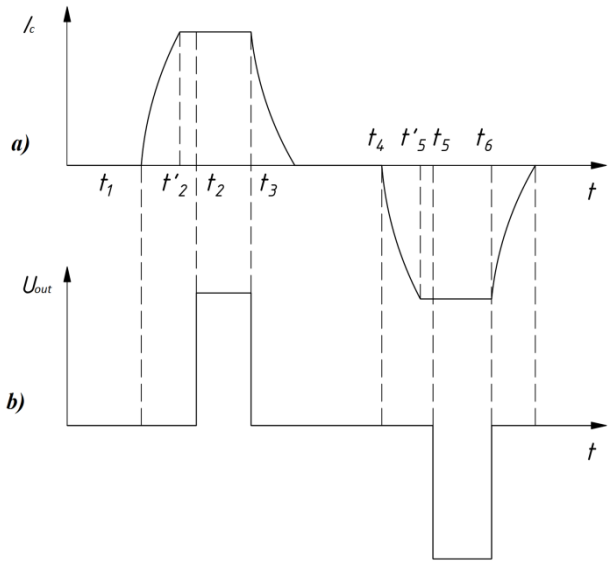

Fig. 1. Timing diagram of the current supply of the inductor and the input signal of the conversion path

The moments t_2 and t_5 correspond to the end of the leading edges of the current pulses of the inductor of positive and negative polarity. In accordance with this, at the intervals from t_2 to t_3 and from t_5 to t_6, the signal is integrated, and the values of $t_3 - t_2$ and $t_6 - t_5$ are selected as multiples of the network period. An integrating ADC can be implemented with an intermediate conversion to frequency or time interval (according to the double integration method [3]). In both cases, the intermediate value will be the value of the signal integral at times t_3, t_6. The values of the integrals for both polarities are summed, and the result of the summation can be attributed to the time t_6. Therefore, the integrated noise values for different polarities, independent of the polarity of the inductor current, should be subtracted from one another. Thus, for the resulting value of the noise $U_{n_{out}}(t)$ at time t_6 we have

$$U_{n_{out}}(t) = \frac{k_0}{\tau}\left[\int_{t_2}^{t_3} U_{n_{in}}(t)dt - \int_{t_5}^{t_6} U_{n_{in}}(t)dt\right], \qquad (3)$$

where $U_{n_{in}}(t)$ is the instantaneous noise voltage brought to the CEM input;

τ is the integration time constant; k_0 is the gain of the conversion path from the CEM input to the integrator input.

In expression (3), the time is counted from the beginning of the period. In the form corresponding to any n^{th} period, it can be written down if we take into account that in this case the argument t_6 will correspond to the instant nT of the end of the nth period:

$$U_{n_{out}}(nT) = \frac{k_0}{\tau}\left[\int_{nT-\frac{T}{2}-t_i}^{nT-T/2} U_{n_{in}}(t)dt - \int_{nT-t_i}^{nT} U_{n_{in}}(t)dt\right] \qquad (4)$$

Where T is the period of the inductor supply current; t_i is the integration time, with $t_i = t_3 - t_2 = t_6 - t_5$

Expression (4) corresponds to samples at times nT of a continuous function of the form

ISSN: 2350-0328

International Journal of Advanced Research in Science, Engineering and Technology

Vol. 6, Issue 8 , August 2019

$$U_{n_{out}}(t) = \frac{k_0}{\tau}\left[\int_{t-\frac{T}{2}-t_i}^{t-T/2} U_{n_{in}}(t)dt - \int_{t-t_i}^{t} U_{n_{in}}(t)dt\right]$$

Expressions (4) and (5) give the same values of the voltage of the noise passing through the transformation path at the moments of the end of each period. Finding the image according to the Laplace function (5) in accordance with the rules of operational calculus, as well as using the operational calculus theorem on delay in the domain of originals and the theorem on splitting a certain integral, you can get the frequency response of the conversion path for noise $G(j\omega)$

$$G(j\omega) = k_0/\tau\,\frac{1}{j\omega}\left[e^{-j\omega\frac{T}{2}} - e^{-j\omega\left(\frac{T}{2}+t_i\right)} - 1 + e^{-j\omega\,t_i}\right] = \frac{k_0}{\tau\frac{1}{j\omega}\left(1-e^{-j\omega\,t_i}\right)\left(1-e^{-j\omega\frac{T}{2}}\right)} \quad (6)$$

The frequency response module | $G(j\omega)$ | determined by taking into account (6)

$$|G(j\omega)| = \frac{2k_0}{\omega\tau}\sqrt{(1-cos\omega t_i)\left(1-cos\omega\frac{T}{2}\right)}. \quad (7)$$

To obtain the frequency response in a form that does not depend on specific times t_i and T, we introduce the reduced frequency Ω

$$\Omega = \omega t_i \quad (9)$$

while $\omega = \frac{T}{2} = m\Omega$,

where$m = \frac{T}{2t_и}$ (9) is a coefficient depending on the ratio of the integration time and the period of the inductor supply.

The expression for the frequency response modulus, relative to the static gain equal to $\frac{2k_0t_i}{\tau}$takes the form

$$|G(\Omega)| = \sqrt{(1-cos\Omega)(1-cosm\Omega)/\Omega} \quad (10)$$

In fig. Figure 2 shows the curves of the frequency response modulus of the conversion path for noise with three values of *m*. From the curves, one can judge the frequency range in which noise with the highest weight passes to the output of the conversion path.

ISSN: 2350-0328
International Journal of Advanced Research in Science, Engineering and Technology
Vol. 6, Issue 8 , August 2019

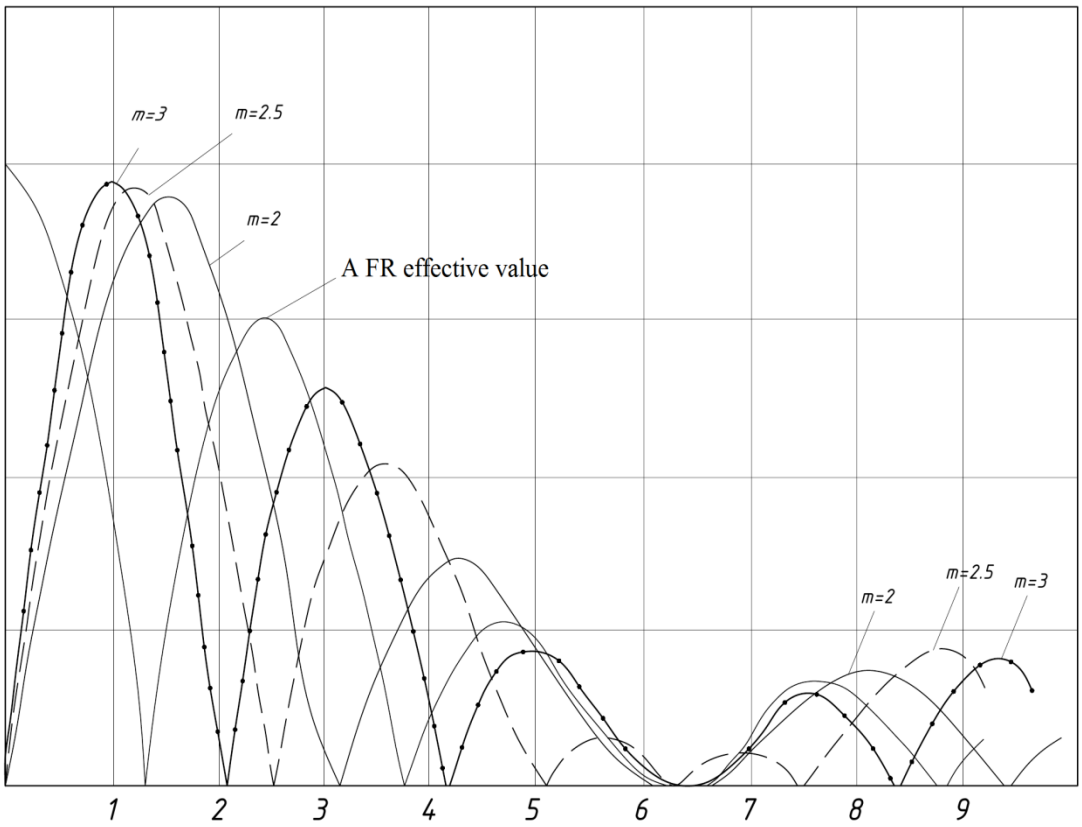

Fig. 2. Frequency characteristics of the conversion path for noise

V. EXPERIMENTAL RESULTS

As can be seen in the figure, the zero-frequency noise component does not pass through the conversion path in contrast to the constant component of the useful signal. This should significantly reduce the passage of flicker noise, the density of which at zero frequency increases indefinitely, which was confirmed experimentally by reducing the frequency $\boldsymbol{\omega}$down to 10^6 C^{-1} [5]. At the same time, from the point of view of passing flicker noise, it is unfavorable to have a maximum frequency response in the low frequency range $\left(\boldsymbol{\Omega = \frac{\pi}{2}}\right)$.

The variance D_{out} (the average square of the effective value of the noise voltage at the output of the conversion path) [4] is determined by the expression

$$\boldsymbol{D_{out} = \int_0^{\infty} |G(j\omega)|^2 S(\omega) d\omega.} \qquad \textbf{(11)}$$

The square root of the variance is the rms effective value of the noise voltage. Dividing this value by the static coefficient of the transmission of the useful signal, we obtain the noise voltage reduced to the input, which is the mean square absolute error of measurement of the CEM input signal.
For white noise with $\boldsymbol{S_w}$ density, taking into account the frequency characteristics (7), (10), relation (11) takes the form

ISSN: 2350-0328

International Journal of Advanced Research in Science, Engineering and Technology

Vol. 6, Issue 8 , August 2019

$$\boldsymbol{D_w = 4k_0{}^2 t_i S_w/\tau^2 \int_0^{\infty} \frac{(1-cos\Omega)(1-cosm\Omega)(d\Omega)}{\Omega^2}};} \qquad (12)$$

for flicker noise density $S_f\omega_0/\omega$-

$$D_f = 4k_0^2 t_i^2 S_f \omega_0/\tau^2 \int_0^{\infty}(1-cos\Omega)(1-cosm\Omega)(d\Omega)/\Omega^3 \qquad (13)$$

To reduce white noise, it is necessary to increase the integration time $\boldsymbol{t_i}$ and that, however, contradicts the speed requirement, since with increasing $\boldsymbol{t_i}$and the inductor feeding period $\boldsymbol{T}$ increases. Since the white noise voltage does not depend on m, it is advisable design the transformation path in such a way that time $\boldsymbol{t_i}$ and takes, perhaps, most of the half of the inductor's power supply period. In this respect, analog-digital pre-formation with intermediate conversion to frequency is preferable, since when converting by double integration, part of half of the period takes the integration interval of the reference signal, thus, at constant $\boldsymbol{T}$, the possible value of $\boldsymbol{t_i}$ decreases.

To reduce the current noise, which is especially important when large $\boldsymbol{R_e}$ is necessary to choose amplifiers with the lowest possible input current.

VI.CONCLUSION AND FUTURE WORK

In conclusion, it can be noted that the results obtained allow us to resolve the contradiction between accuracy and power consumption by optimal selection of the method and parameters of the analog-to-digital conversion and the type of the input operational amplifier.

Currently, these data are taken into account when developing a promising series of electromagnetic flowmeters

REFERENCES

[1]Zvenigorodsky E.G., Lebedev S.M. The concept of building a unified series of promising electromagnetic microprocessor flowmeters. Design features. Collection of scientific papers.Industrial methods for measuring the flow of liquid and gas. M.1988

[2]Jumaev O.A., Abdujalilov A.O. Mathematical Modeling of Intelligent Measurement Systems.International Journal for Research in Applied Science & Engineering Technology. Issue IV, April 2019.